Computational Design and Robotic Fabrication of Dry-Stacked non-standard spanning Limestone Assemblies

Chin-Lun Lu
University College London
Zhenghao Zhu
University College London
Guillem Perutxet Olesti
ucbqgpe@ucl.ac.uk
University College London
Peter Scully
University College London
Pradeep Devadass
University College London

Research Article

Keywords: Non-standard materials, Material Computation, 3D Scanning, Multi-Objective Optimization, Robotic Fabrication

Posted Date: November 20th, 2025

DOI: https://doi.org/10.21203/rs.3.rs-8019586/v1

Additional Declarations: No competing interests reported.

Computational Design and Robotic Fabrication of Dry-Stacked non-standard spanning Limestone Assemblies

Abstract

Natural stone, an abundant and low-carbon material, often generates substantial unusable waste through quarrying and masonry processes, including rubble, offcuts, and irregular fragments. While there is growing interest in repurposing these byproducts, their non-standard and irregular geometries pose major challenges for integration, restricting their use in architecture primarily to cladding, flooring, and other non-structural applications. Finding innovative applications for this waste could help revive the use of stone in construction while further lowering its environmental impact. This study introduces a workflow to optimize the geometry of non-standard stone blocks through minimal modifications, enabling construction with highly variable, locally sourced material. The proposed methodology consists of a heuristic generative algorithm based on a library of 3D scanned limestone blocks and guided by a pre-defined global geometry. This enables a data-driven model for the targeted modification of joints between blocks through robotic machining. In turn, robotic machining is thereby optimized to save energy and time. This approach was validated through the fabrication of 18 stones, which were assembled into a three-legged arch, demonstrating the feasibility of using non-standard stone for architectural structural applications.

Keywords: Non-standard materials, Material Computation, 3D Scanning, Multi-Objective Optimization, Robotic Fabrication

1 Introduction

Natural stone

The use of natural stone as a structural construction material has gained renewed traction in recent years, driven by both environmental imperatives and advances in digital fabrication (1). Stone offers a materially and environmentally robust solution for contemporary architecture when reintroduced as a primary structural component (2). Its high compressive strength, dimensional stability, and long-term durability make it particularly suitable for load-bearing applications such as walls, columns, and vaulted systems (3). Stone occurs as a ready to use product, where its carbon emissions result from the energy to quarry, process, and transport the material (4). Unlike concrete and steel, stone requires relatively minimal processing and does not require high-temperature or chemically transformative manufacturing. Furthermore, stone is abundantly available, has the potential to be sourced locally, and has immense potential for reuse as a fully reversible construction material, particularly when integrated into non-destructive reuse assembly systems, such as dry-assembly systems (5). This practice of reuse was common in ancient times, best exemplified in *spolia*, and represents a shift from the exploitation of the geo-ecosphere towards the utilization of the anthroposphere, which includes existing building stock(6).

1. 1 Decline of natural stone

Despite its potential, the use of stone as a primary structural material declined with the rise of more cost-effective and versatile alternatives such as concrete and steel. In the modern era, their dominance has been further reinforced by standardized production methods, established global supply chains, and economies of scale. This shift was precipitated by industrialization and globalization, which together fostered a construction industry increasingly oriented toward mass production, rapid deployment, and uniformity of materials. The expansion of cost-effective transportation infrastructure and reduced logistical barriers to distributing industrial materials across vast distances, giving rise to centralized industrial production and leading to gradual disappearance of local quarries, a critical factor to ensure stone's affordability and widespread use (1). At the same time, rising labor costs and the transition to industrialized construction methods, diminished the competitiveness of stone as an economically viable material. These developments reflect broader dynamics associated with extractive economies of growth, in which natural materials are evaluated primarily through the lens of economic efficiency rather than environmental, cultural, or artisanal value. Consequently, stone has become largely relegated to cladding or decorative applications in contemporary architectural practice (4).

1. 2 Stone waste streams

Circular design with natural stone presents emerging opportunities for the reuse of the various waste streams generated at the various stages of natural stone processing in pursuit of standardized materials and dimensions (7).

Waste in the stone industry arises primarily at two stages: selection and dimensioning (8). Since each block possesses unique geometric and geological characteristics, much of it fails to meet the narrow specifications required for dimension stone and ultimately for standardized stone products. This leads to high rejection rates in order to conform to design systems that prioritize geometric uniformity. Furthermore, natural stone blocks that exhibit irregular shapes, fractures, or visual inconsistencies are often discarded despite being structurally sound (9).

Further material loss occurs during the dimensioning phase, when selected blocks are cut, shaped, and finished to produce standardized forms. Sawing generates kerf waste and offcuts, while finishing processes produce slurry and fine particulate debris which is often unrecovered. The pursuit of flat faces and precise dimensions results in the removal of considerable volumes of usable stone. Together, these practices reflect an industrial model that favours uniformity over adaptability, yet they also highlight significant untapped potential for reuse and innovation (10).

Non-standard materials

In recent years, the Architecture, Engineering, and Construction (AEC) industry has increasingly turned toward circular design practices, prompting a growing interest in the use of non-standard, minimally processed, and reclaimed materials. Central to this shift is the role of computational design, which is emerging as a strategic tool for enabling circular construction by aligning architectural and structural decision-making with the availability and characteristics of existing material stocks (7,11). By embedding material availability particularly that of irregular or reclaimed components into the early stages of the design process, it becomes possible to close material loops and reduce dependence on standardized, resource-intensive systems. This reframes design not merely as a formal or functional exercise, but as a critical mediator between material constraints and construction outcomes. As a result, architectural practice has increasingly moved away from artificial geometric precision toward approaches that embrace the inherent variability of natural and reclaimed materials, fostering local sourcing, material reuse, and significant waste reduction. Computational methods, particularly parametric and generative design tools combined with optimization algorithms, are essential to making this transition scalable. These tools can automate the otherwise extremely complex process of working with non-standard elements by interpreting large material datasets and generating design solutions that efficiently allocate available resources.

At the core of the inefficiencies associated with circular stone construction lies the challenge of indeterminacy through the inherent variability in shape, size, composition and structural properties that characterizes minimally processed or reclaimed stone (12). Irregular geometries challenge conventional modeling tools, require adaptable fabrication tools, and complicate the prediction and verification of structural performance. Recent advancements in computational design, digital fabrication, robotic automation, and vision-based systems have begun to overcome these limitations. These technologies now enable to work effectively with irregular, non-standard elements and open new possibilities for incorporating waste streams from natural stone processing into circular construction workflows. To harness

the ecological and architectural potential of highly variable stone, new strategies are needed that can transform non-standard material stocks into structurally coherent assemblies, not by eliminating variability, but by making it legible, manageable, and even advantageous within a digitally mediated construction process.

1. 3 State-of-the-art

Previous work in the field of non-standard computer aided design and manufacturing have explored various methods to capture, process and assemble, geometry acquisition, generative design and structural algorithms and digital manufacturing tools with various materials in various degrees and strategies of processing for assembly. The Woodchip Barn creates an arch structure from a set of curated timber forks which are 3D scanned and assembled through custom robotically machined joints. In addition, this project demonstrates material-aware design through the leveraging of the anisotropic structural properties in conserving the timber grain intact (13). Knippers et al. demonstrate a generative algorithm and adaptable robotic fabrication methodology for the design and manufacture of corrugated shell structures from folded sheet metal of non-standard geometries and properties, in which the design output conforms to material availability (12). In the realm of non-standard stone construction, the project Cyclopean Cannibalism develops a compound curvature wall through the nesting of quasi-planar polygonal rubble stones through a 3D scanning, a recursive algorithm, a combination of robotic sawing and milling, and manual dry-assembly. This approach requires the machining of all 4 interfacing faces in the assembly, yet achieves to make use of 73% of the scanned stone material (14). Autonomous dry stone presents a method to construct dry stone walls in situ using completely unmodified natural stone, facilitated by a customized autonomous mobile hydraulic excavator. Terrain mapping, and stone localization and digitization are performed by cabin-mounted LiDAR sensors and planning is performed on-the-fly (14,15).

These case studies highlight three core challenges in robotic fabrication with irregular materials: managing the complexity of multi-scalar sets of materials, developing rational aggregation strategies for spanning stone structures, balancing selection process and geometry processing to meet design and structural targets.

1. 4 Research

This research presents a material-driven digital manufacturing workflow that integrates computational design, 3D scanning, and robotic fabrication to enable the heuristic assembly of irregular limestone rubble through custom joints to create spanning structures through utilization of minimal energy for processing and machining. Beginning with structured light scanning of a curated set of stones, high-resolution mesh models were generated and organized into a custom database. A generative algorithm then analyzed and ranked potential face-to-face configurations based on geometric compatibility, identifying optimal connections and determining which contact surfaces required intervention. The algorithm

optimized the position of the stones based minimal machining while ensuring structural stability. Flat interface surfaces were algorithmically generated and selectively milled onto the stones using robotic subtractive manufacturing techniques, minimizing material processing while enhancing assembly precision and stability. The processed elements were assembled into a dry-laid, three-legged arch structure, allowing for full-scale evaluation of spatial and structural performance. This selective intervention approach targeting only essential contact areas offers a pragmatic alternative to fully autonomous systems, by balancing robotic adaptability with material efficiency, structural clarity, and design control. The result is a scalable strategy that preserves the expressive character of irregular stone while reducing computational complexity and supporting sustainable construction practices through minimal waste and maximal reuse. Minimal modification is often required in architectural applications such as walls, roofs, and columns at a building scale, where unmodified stone cannot ensure precise load transfer, stability, or alignment, although it remains suitable for larger infrastructural projects such as retaining walls or sea defences. At the building scale, the degree of selective modification becomes critical, allowing irregular stone to achieve structural reliability while maintaining its natural aesthetic character.

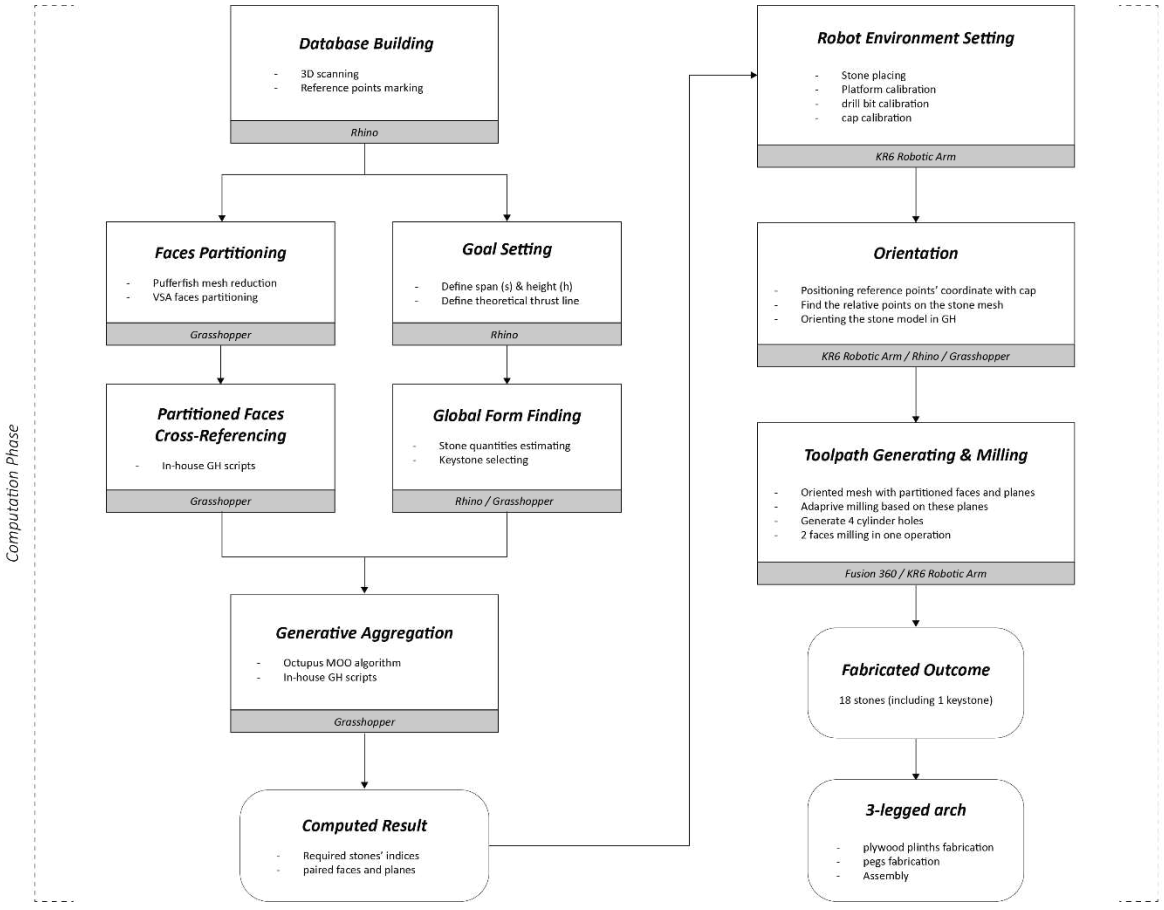

Figure 1. The flowchart of the overall workflow.

2 Methods

This research proposes a method for facilitating the robotic assembly of irregular limestone blocks by introducing minimal surface modifications. The process comprises (1) development of a global assembly geometry, (2) 3D scanning and digital library creation of available stones, (3) development of a matching algorithm to identify optimal stone pairings and required modifications, and (4) execution of these modifications via robotic milling.

2.1 Global geometry design

First, a target global geometry was established to guide the heuristic processes of stone selection, modification, and assembly. In this study, the global geometry was defined as a three-legged arch composed of a continuous sequence of interlocking stone units, arranged to approximate a ruled surface with three contact points on the ground plane (Figure 2), providing a suitable structure to test both architectural expression and structural. Unlike a volumetric geometry, this approach reduces the computational complexity to a two-dimensional problem, requiring only two faces per block to be considered for stone-to-stone connections during assembly. All cross-referencing and machining operations were aligned with this predefined geometry, ensuring that local decisions contributed coherently to the final assembled structure.

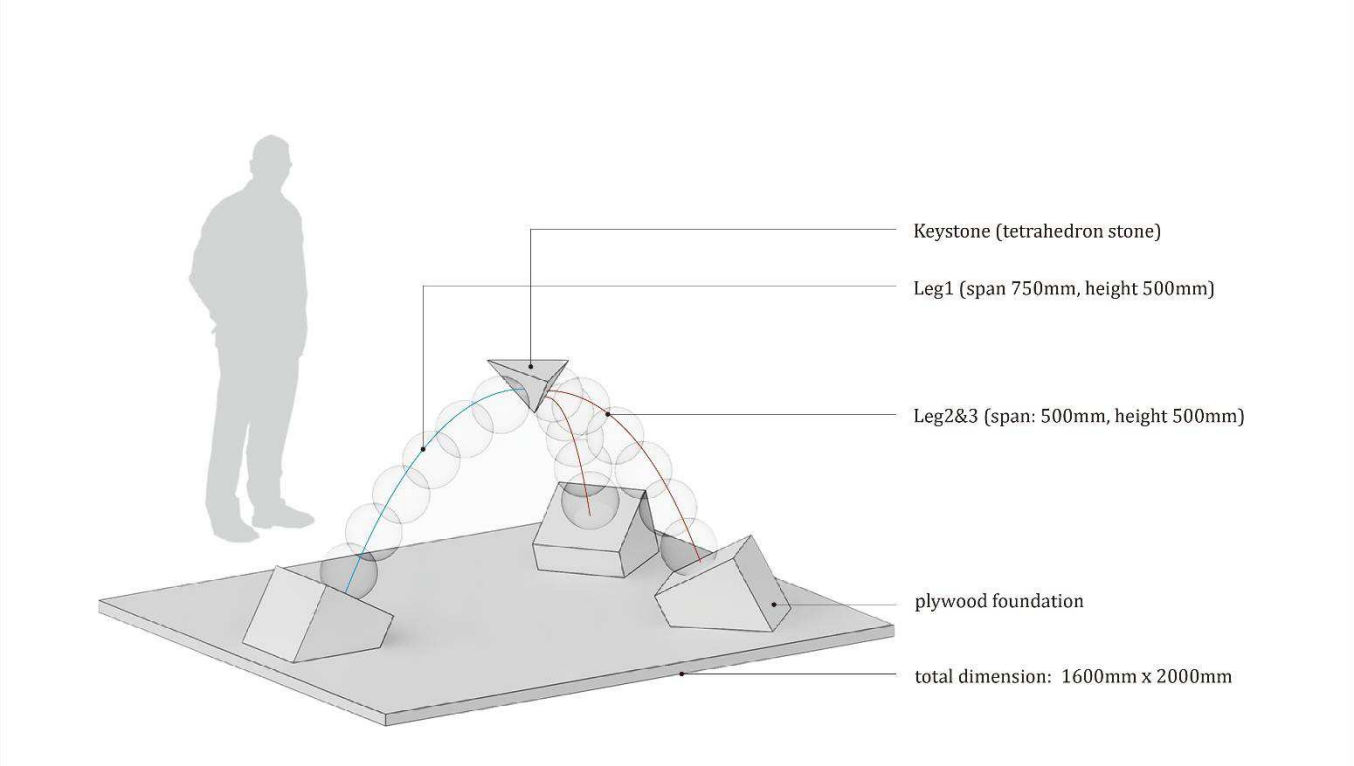

Figure 2. Global form finding: concept diagram of the 3-legged arch global design.

Assuming uniform stone density, weight, and size, a theoretical thrust line was predefined as a parabolic curve interpolated using two primary parameters: span and height. Stones were aggregated along this curve to ensure the structural stability of the assembly (Figures 3a). Structural stability was evaluated by measuring the distance between each stone's centre of gravity (Cg) and the theoretical thrust line. A smaller distance deviation indicates a more stable configuration, as the load path remains closer to the optimal structural alignment.

From a sectional perspective, the overlapping volumes between adjacent stones were trimmed using a series of clipping planes. These planes were aligned perpendicular to the side elevation of the assembly. As a result, a specific angular relationship existed between consecutive clipping planes, meaning the stones could not rotate arbitrarily any rotation would misalign the planes and compromise the intended fit. By manipulating these angles, the curvature of the arch could be controlled, allowing the assembly to conform to the target geometric configuration (Figure 3b, 3c).

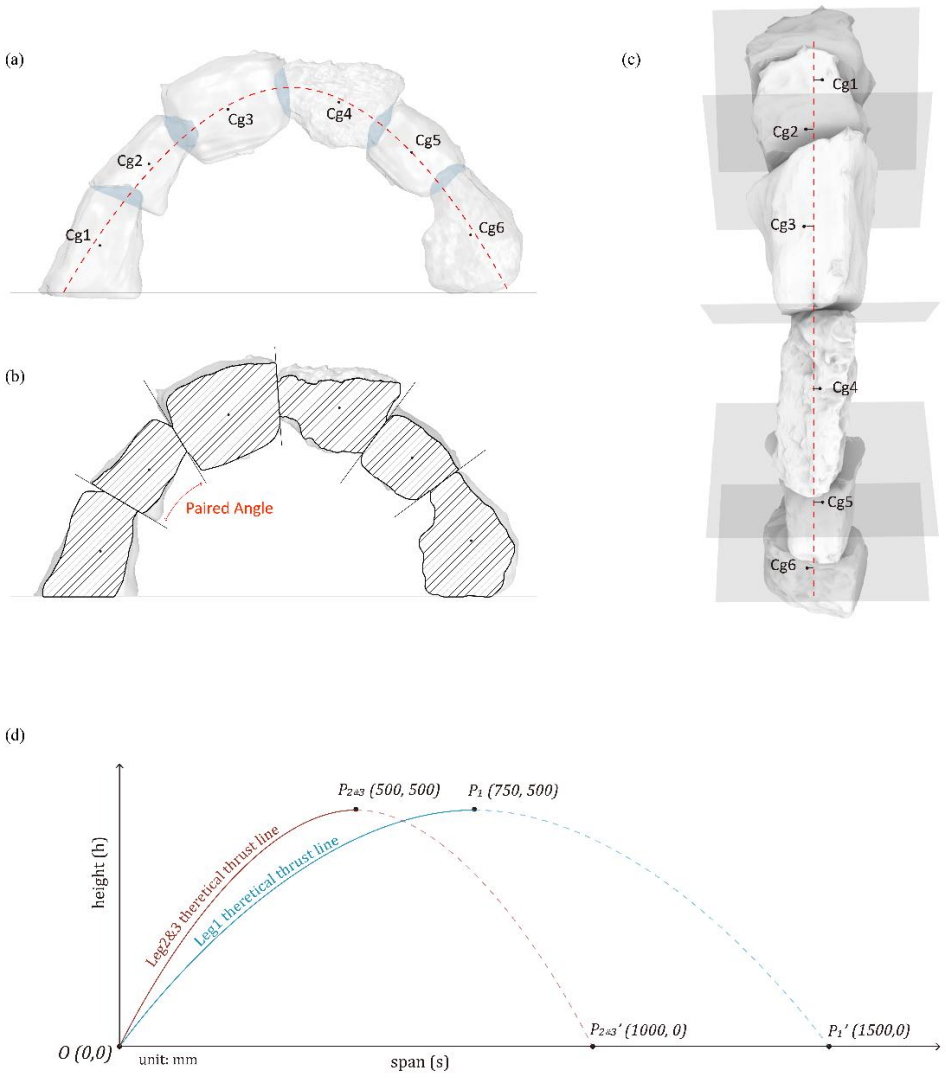

Figure 3. Concept of linear stone arch structure. (a) Draw a theoretical thrust line as a basis of stone aggregation (b) The section with the planes aligned. (c) The top view, the deviation between center of gravity (Cg) and theoretical thrust line. (d) Predefine the theoretical thrust line with interpolated parabolic curve.

2.2 3D scanning and Database Development

A total of 50 irregular limestone rubble fragments were 3D scanned to construct a digital mesh database for computational analysis and robotic fabrication. Scanning was conducted using a handheld Creaform structured light scanner in combination with a turntable to ensure full surface coverage. A resolution of 0.2 mm was used to balance geometric detail and file manageability. Each stone was marked with small, drilled reference points prior to scanning to allow for alignment between digital and physical coordinates during robotic milling.

2.3 Planar segmentation via Variational Shape Approximation

To enable geometric analysis and pairing of irregular stone surfaces, a face segmentation algorithm was developed using the Variational Shape Approximation (VSA) method (16), implemented in Grasshopper via a custom Python script. VSA was selected for its ability to reduce complex mesh geometries into a manageable number of locally planar regions, while preserving critical geometric features relevant to fabrication and assembly.

The algorithm operates by analyzing surface curvature and clustering mesh faces into regions with minimal deviation from planarity. Each high-resolution scan is thus approximated by a set of quasi-planar patches, which are extracted based on local normal consistency and surface flatness. These regions serve as candidate connection faces, simplifying the comparison and matching of stones for assembly.

The resulting output is a simplified, polygonal representation of each stone that retains its overall topology while abstracting away unnecessary geometric detail. In addition to the segmented faces, each mesh also contains embedded reference markers to ensure correspondence between digital geometry and physical stone positioning during robotic milling.

This partitioned dataset served as the foundation for all subsequent processes, including face matching, machining constraint evaluation, and keystone selection. In particular, stones segmented into a tetrahedral-like configuration, characterized by three diverging planar faces, were prioritized as keystone candidates for the three-legged digital arch. This configuration provided a stable anchor point for distributing curvature and orientation across the assembly.

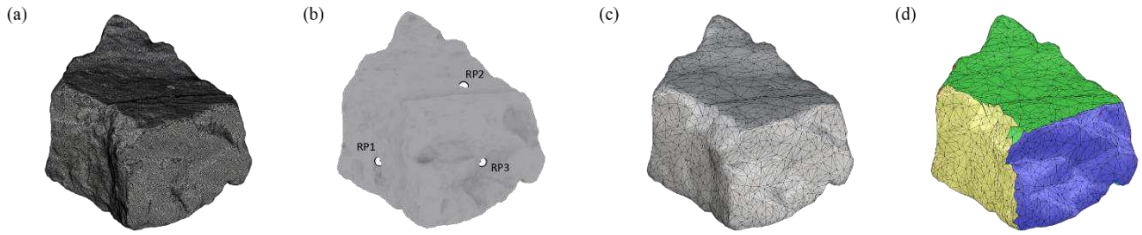

Figure 4. (a) High-resolution 3D scanned mesh. (b) Labelling reference points on the predrilled holes. (c) Simplified mesh by Pufferfish (d) Partitioned mesh by Variational Shape Approximation.

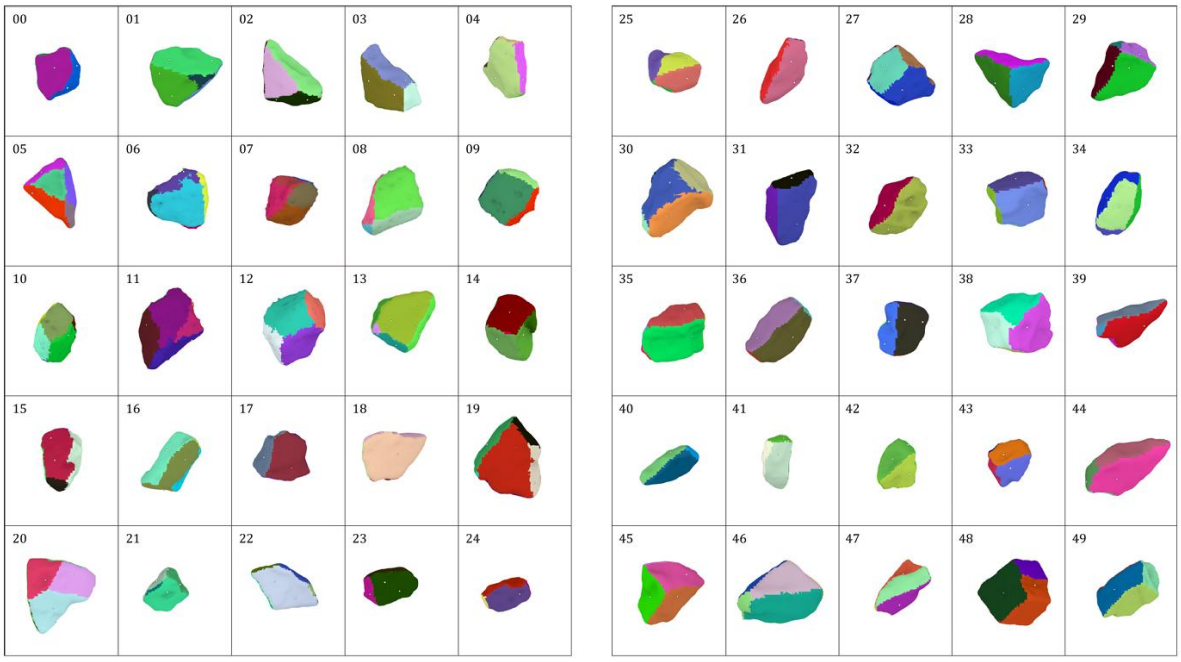

Figure 5. The database of simplified scanned meshes with color-coded face partitions.

2.4 Face library evaluation

Building upon the previously identified quasi-planar regions from VSA segmentation, a second algorithm was developed to evaluate and orient candidate stone pairs in alignment with a predefined digital thrust line. This process aimed to identify stone connections that both followed the global curvature and minimized material intervention.

2.4.1 Surface area

Before evaluating internal angle, we filter out faces whose areas are too small (less than 15,000 mm²) to provide structural stability. (Figure 6) This area threshold is determined based on the required contact surface for assembly.

Figure 6. (a) The structure without area filtering exhibits a tiptoe-like stance, which is unstable. (b) After removing smaller-area faces, the aggregation shows improved structural stability.

2.4.2 Internal angles

For each stone, all angular relationships between internal planar face pairs and surface area were evaluated. Internal angles, derived from, served as a primary metric for assessing geometric compatibility. A custom Grasshopper script systematically cross-referenced all possible face pair combinations within each stone, by calculating the cross product of the surface normal of face pairs. The output is a dataset of internal angular relationships (Figure 7).

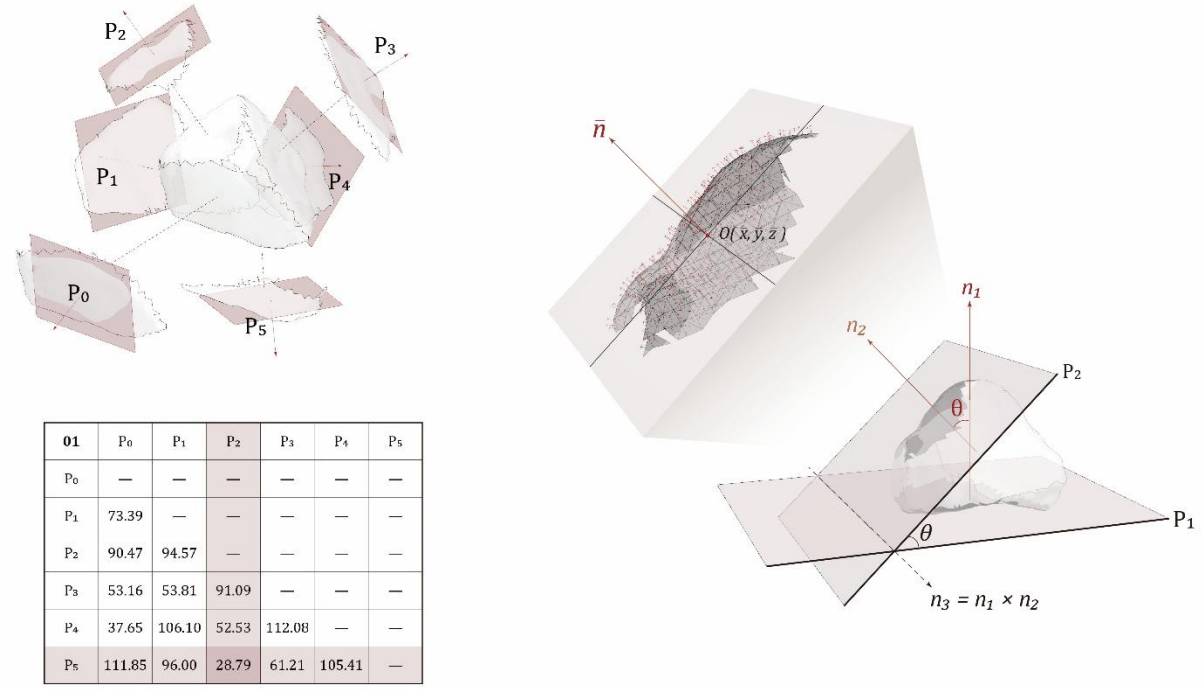

01	P0	P1	P2	P3	P4	P5
P0	—	—	—	—	—	—
P1	73.39	—	—	—	—	—
P2	90.47	94.57	—	—	—	—
P3	53.16	53.81	91.09	—	—	—
P4	37.65	106.10	52.53	112.08	—	—
P5	111.85	96.00	28.79	61.21	105.41	—

Figure 7. The illustration of partitioned faces and their mean planes. The chart shows the degree result of mean plane cross-referencing. In this chart, the smallest angle is 28.79°, formed by planes P2 and P5. The definition of the mean plane on the partitioned face, with

the illustration of the angle (θ) between two mean planes.

Generally, stones with smaller angles are more suitable for use. By cross-referencing table, we can identify the smallest angle for each stone (Figure 8). Once the smallest angle of each stone is known, we sort all the stones in ascending order based on their minimum angle.

Since an excessive number of stones with large angles may lead to over-curling, we remove those with the largest angles from the dataset. (Figure 8) Specifically, we retain only the top 70% of stones with the smallest angles to serve as the input for the next step in the generative algorithm. In the other words, only 35 stones are chosen. (Figure 9) Similar to the previous area filtering step, this larger angle filtering also helps reduce computational load.

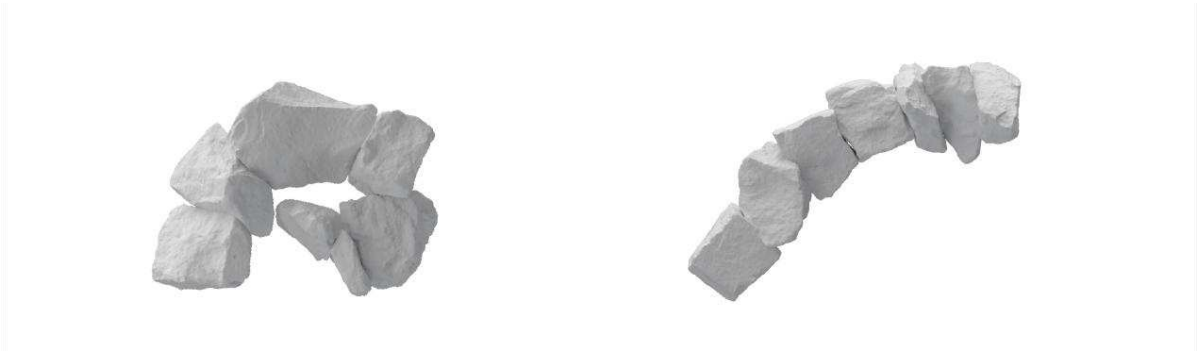

Figure 8 (a) The structure without angle filtering exhibits over-curling. (b) Using stones with smaller angles increases the likelihood of reaching the target cumulative angle.

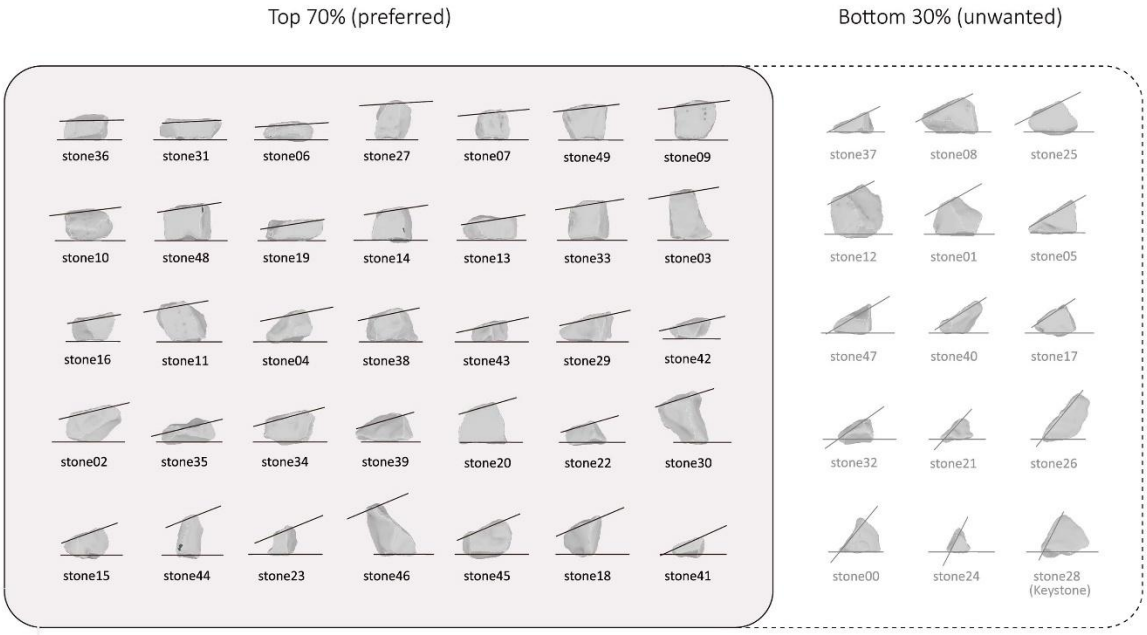

Figure 9. The list of minimum angles of stones. Remove the bottom 30% stone from database.

2.4.3 Alignment optimization

To further streamline face alignment, the central point of each planar face was used as a reference for connection. During digital placement, stones were oriented such that the connection between two faces followed the average rotation between their normals. This constraint simplified alignment by approximating connections as straight lines in side view (Figure 2b), reducing rotational variability and narrowing the algorithm's search space.

2.5 Generative Aggregation

To estimate the number of stones needed, we first measured the total length of the intended thrust line and approximated how many stones would be required to fill that length by using spherical proxies whose volumes matched the average volume of the scanned stones (Figure 10)

By adjusting the volume of overlapping between spheres, the estimated number of stones becomes a flexible value, indicating a reasonable approximate range that is used as input for further computation. At the same time, we also obtain the target cumulative angle (θ) to serve as the objective of the computation.

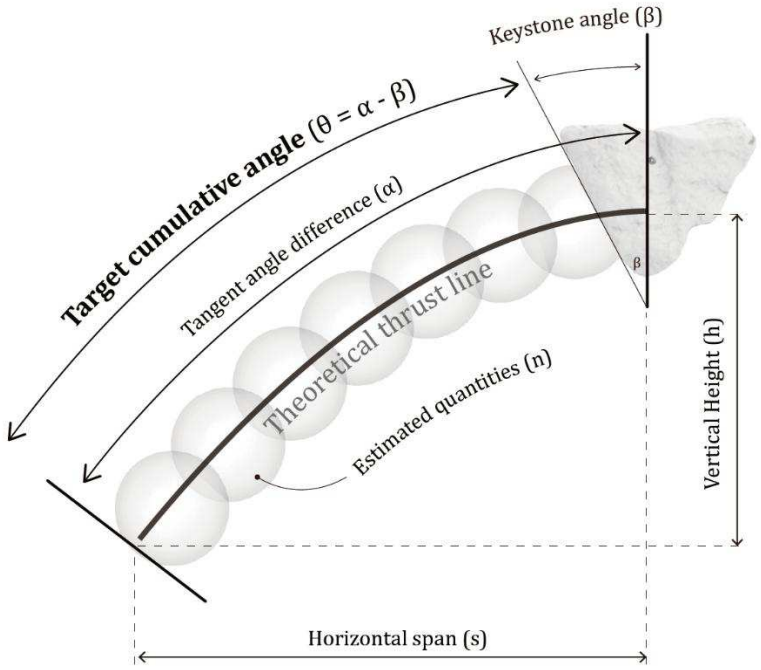

Figure 10. The illustration of the angular relationships between aggregated stones and the keystone. To simplify estimation and analysis, each stone is represented by a sphere of

equivalent volume. (This chart has been changed)

After identifying the filtered list of smallest internal angle for each stone, we proceeded to search for combinations of stones that satisfied the structural requirements of the arch. This process was guided by three primary variables: stone index, quantity, and sequence. (Figure11).

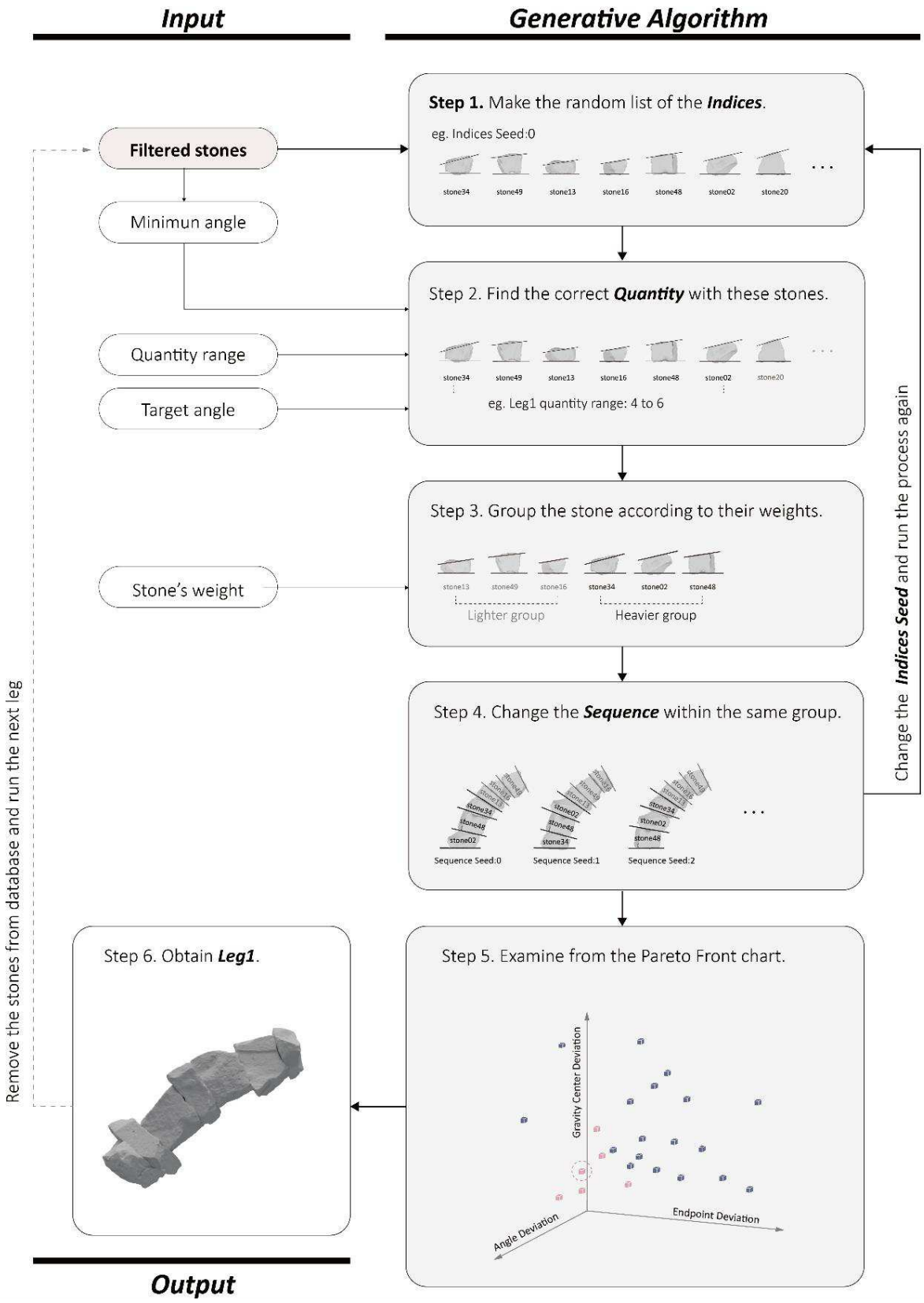

Figure 11. The flow chart illustrates the logic of the generative aggregation algorithm.

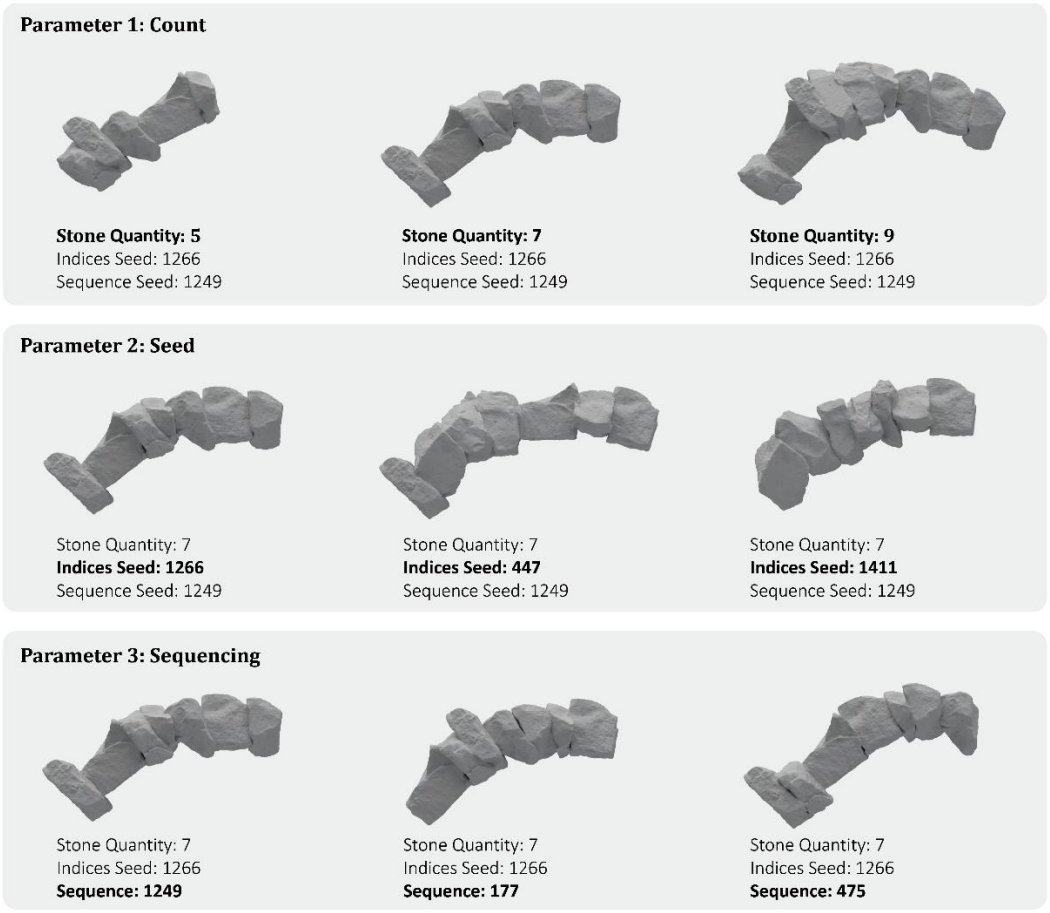

Figure 12. The different results by changing three parameters: *quantity, index,* and *sequence*.

Taking the computation of the first leg as an example:

(1) Firstly, a random list is generated from the 35 filtered stones. As the random seed changes, the order of the stone indices also varies.

(2) Secondly, based on the estimated quantity range and the target cumulative angle, a specific number of stones can be calculated. In simpler terms, these first two steps involve randomly selecting 4 to 6 stones from the 35 candidates to form a combination that approximates the target angle.

(3) Thirdly, *grouping*, stones were sorted into weight-based groups, with heavier stones prioritized for lower positions in the structure and lighter stones placed above. This not only improved force distribution but also narrowed the range of permutation possibilities during optimization.

(4) Randomly change the sequence of stones within the same group. The sequence in which the stones were arranged had a significant impact on the final geometry.

Since each stone has two potential connection faces and can be flipped in orientation, the number of possible configurations expanded rapidly. To address this issue, each stone was constrained in a single direction, eliminating the option to flip stones during the aggregation process.

(5) By running simulations with varying combinations of the three key parameters quantity, index, and sequence across multiple random seeds, a wide range of aggregation outcomes was generated. To evaluate and identify the most structurally viable configuration, we employed multi-objective optimization (MOO) using *Octopus*, a Grasshopper plug-in based on genetic algorithms. This approach enabled the comparison of each outcome against a defined set of performance criteria, helping to balance competing constraints through iterative selection. The optimization was guided by three primary objectives.

- Angle deviation measures the difference between the target cumulative angle and the sum of the actual face-pair angles within the selected stone set; lower deviation indicates a closer match to the intended keystone alignment. Second,
- Gravity center deviation quantifies the shortest distance between the center of mass and the reference catenary curve, with smaller values suggesting better alignment with the ideal structural thrust path.
- Endpoint deviation evaluates the distance between the terminal point of the assembled structure and the designed endpoint of the thrust line, which is critical to ensuring that the full arch span and height are achieved to support the keystone effectively (Figure 11).

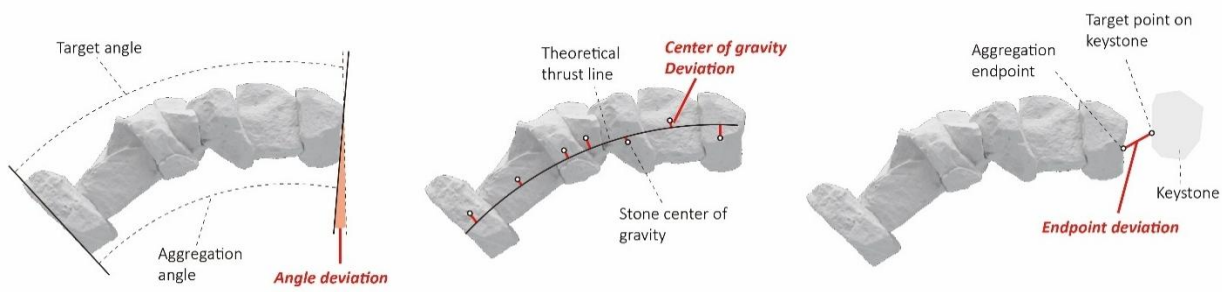

Figure 13. The illustration of three objectives for MOO.

The outcomes of the MOO process are presented as a Cartesian plot of deviations for the three defined objectives, commonly referred to as the Pareto Front (Figure 12). Several options appear near the origin of the Cartesian diagram and can be considered as potential candidates. Among these, one option is manually selected based on its overall reasonableness, and is identified as the best-fit result. Once the optimal aggregation is

selected, the corresponding stone indices are removed from the database. The algorithm is then re-run with the updated dataset to generate the remaining two arch legs (Figure 12).

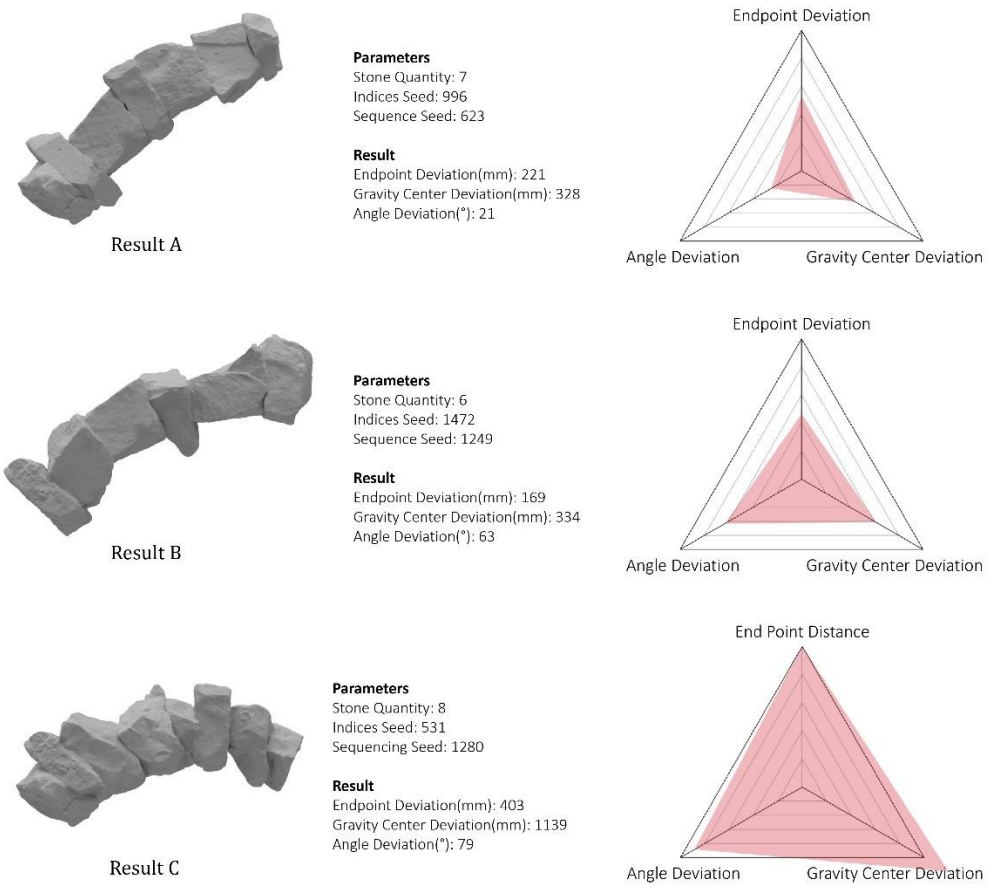

Figure 14. The results analysis from MOO. The smaller area of triangle shows the less deviation of three parameters, which can be selected as the best-fit.

2.6 Robotic Fabrication

Following the computational selection of stone indices and corresponding face pairs for the three-legged digital arch, the fabrication phase was carried out using robotic milling. The robotic fabrication set-up consisted of a Kuka KR6 robotic arm with a Draper router with a 13.4mm brazed diamond end mill. All machining operations were performed as dry machining and no coolant was used during the cutting operations. This stage translated the digital assembly geometry into precise physical modifications on each stone unit.

3.6.1 Irregular Stone workholding

One of the primary challenges in robotic milling of unprocessed limestone rubble lies in securely fixturing non-standard, irregular geometries. To address this, a custom fixturing platform was developed, capable of supporting a wide variety of stone shapes without

requiring custom jigs for each unit. The setup utilizes three adjustable support pins arranged in a triangular configuration to elevate and stabilize the stone, along with a movable clamping mechanism to fix the piece in place during milling operations (Figure 15). This configuration offers both flexibility and repeatability, enabling reliable access to the intended machining faces while avoiding the need to reorient or flip the stone mid-process, which would introduce error.

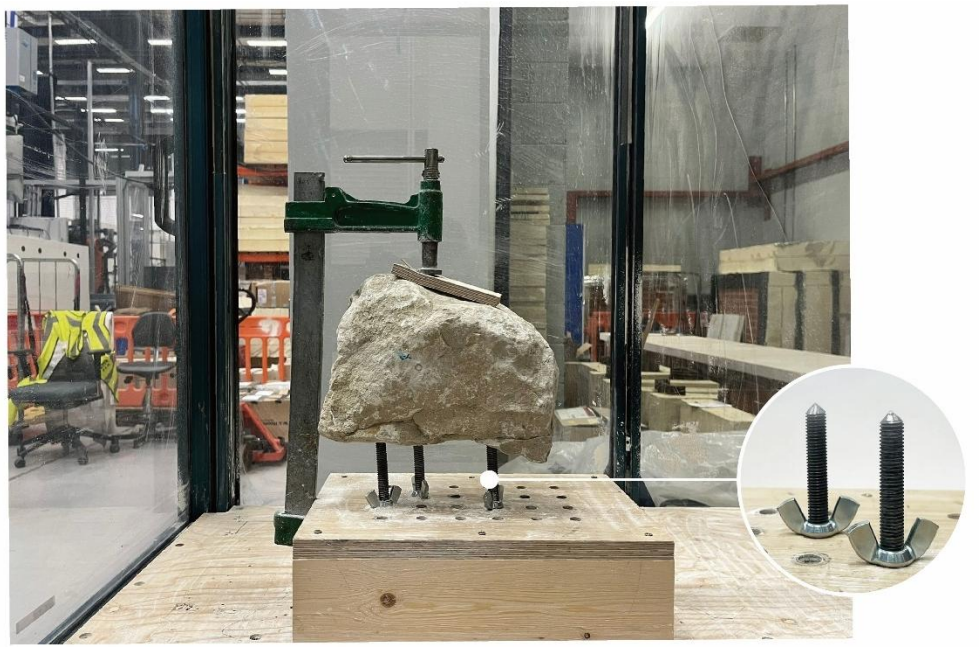

Figure 15. The modular work holding solution for irregular stones.

3.6.2 Workobject calibration

To ensure precise correlation between digital toolpaths and physical stones, each stone was pre-drilled with three reference markers prior to 3D scanning. These markers were used for three-point spatial calibration, allowing for accurate registration of the stone's real-world orientation and position in the robotic workspace. This alignment process ensured that milling operations matched the intended geometry derived from digital modeling (Figures 14–15).

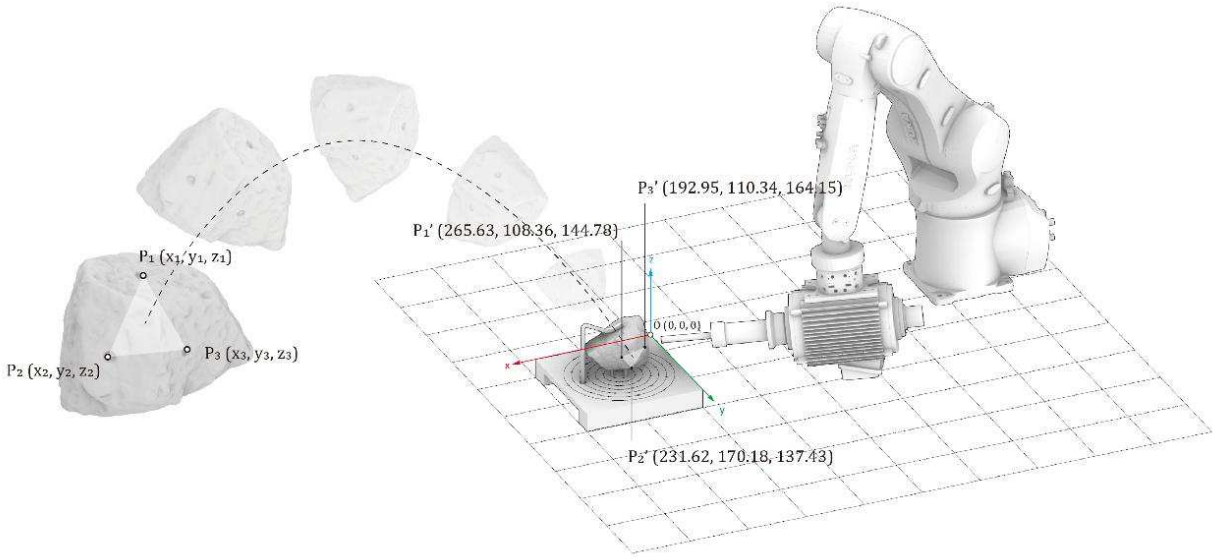

Figure 16. Orient the stone according to the points coordinate on the 3D model environment for the later toolpath generation.

3.6.3 Toolpath Generation and machining operation

Toolpaths were developed using Autodesk Fusion 360, based on the segmented face geometries generated during the computational phase (Figure 16). For each stone, the robotic milling operation consisted of:

- Milling two flat faces to enable accurate stone-to-stone connections.
- Drilling four holes per face to accommodate steel pegs that enhance mechanical interlock.

A *flat parallel* strategy was selected for machining the stone surface. This strategy was chosen because it produces a consistent, uniform toolpath that follows the part's surface contours in evenly spaced passes and provides a good balance between surface quality and machining efficiency.

A **13.4 mm diameter endmill** was used to ensure adequate tool rigidity and surface coverage. The larger tool diameter helps to withstand the high cutting forces encountered in stone machining, while also increasing the material removal rate compared to smaller cutters.

The **10 mm stepover** was chosen to reduce machining time while maintaining a smooth surface finish quality.

The **1 mm stepdown** was selected to control cutting forces and limit the risk of tool or material fracture. Stone is a brittle material, so shallow stepdowns help prevent chipping by keeping the engagement forces low and consistent across layers. This conservative depth of cut also helps maintain dimensional accuracy and extends tool life.

The **feedrate** was set to **20 mm/s (1200 mm/min)** to maintain stable cutting conditions during dry machining of the stone. Since no coolant or lubricant was used, heat dissipation relied entirely on the tool and the surrounding air. A slower feedrate helped to limit the generation of excessive frictional heat, which could otherwise cause localized thermal damage to the stone surface or accelerate tool wear.

At the same time, this feedrate provided a balanced compromise between machining time and tool longevity. Higher feedrates under dry conditions would increase the risk of chipping, vibration, and premature edge degradation due to insufficient cooling. By maintaining a moderate feedrate, cutting forces remained consistent and manageable, ensuring smoother tool engagement and improved surface integrity.

During the machining process, the stone is continuously subjected to the pushing force of the tool, causing it to vibrate and shake. Over time, this may lead to positional displacement, which can affect machining accuracy. To monitor this, a pressure gauge is placed on the back side of the machined surface to measure whether the stone appears any noticeable movement. (Figure 17) If a noticeable displacement is detected, the aforementioned machining parameters will be adjusted immediately to reduce the impact on the stone (for example, by decreasing the stepover, stepdown, or feed rate).

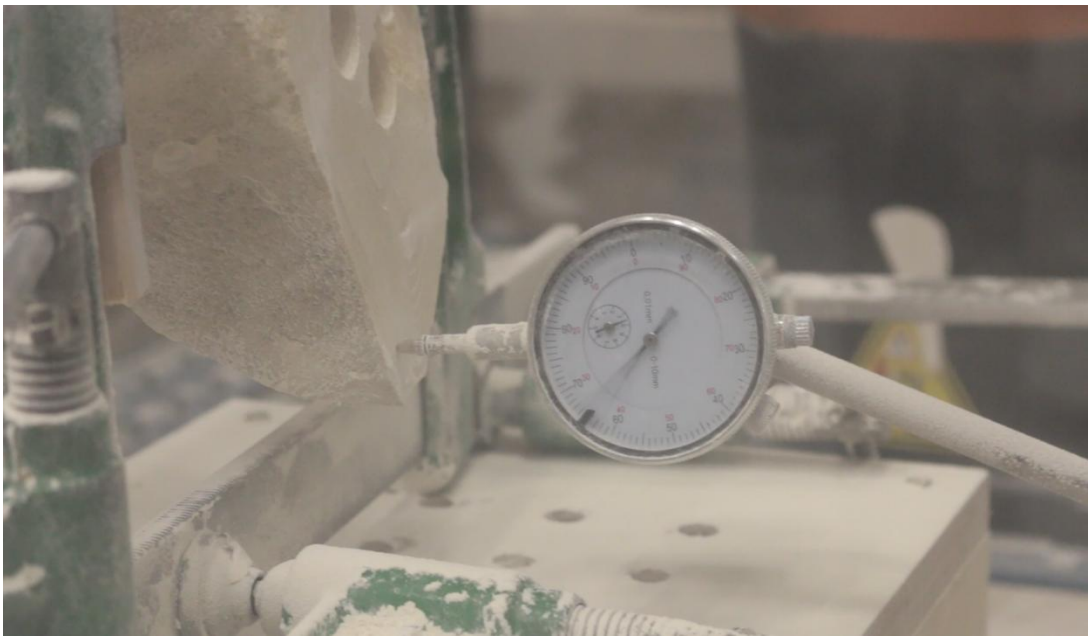

Figure 17. The pressure gauge could be used to detect the displacement.

3.6.4 Physical assembly

The final structure was assembled manually and consisted of a three-legged arch composed of 18 robotically milled limestone blocks, each positioned according to its digitally computed placement and orientation. The arch legs rested on custom CNC-cut plywood plinths, designed to provide consistent base support and precise alignment at each leg's contact point

with the ground. Assembly was carried out without adhesives or mortar, relying instead on the precision-milled planar faces and a system of steel pegs to ensure proper alignment and mechanical interlock.

Each mating face included four embedded steel pegs (Figure 18), which not only simplified alignment during assembly but also significantly increased resistance to shear forces and rotational slippage. This passive mechanical reinforcement strategy enhanced the overall stability and robustness of the structure while remaining consistent with the project's aim of minimal material intervention. The result was a materially efficient, structurally coherent assembly that faithfully translated its digital counterpart into built form.

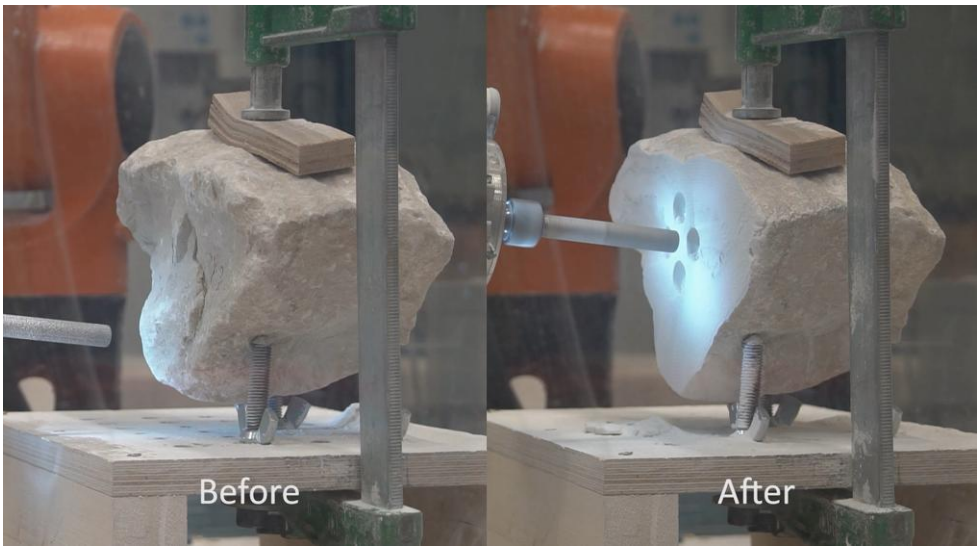

Figure 18. Before and after the machining process.

Figure 19. The final outcome: three-legged arch.

3 Results and Discussion

The project successfully resulted in the fabrication and assembly of a three-legged dry-stacked arch, consisting of 18 limestone blocks, including a central keystone. These stones were mounted on top of custom-made plywood plinths, which were securely anchored to the ground to provide a stable foundation during and after construction (Figures 18 & 19). Each stone retained the majority of its natural form, with only two planar faces per block selectively machined to create custom joints. This minimal intervention approach enabled precise assembly while minimizing waste in processing.

The robotic milling process, guided by digital toolpaths generated in Fusion 360, achieved high levels of surface accuracy. A reduced stepover distance was employed during milling to eliminate visible toolpath artifacts, producing smooth, planar surfaces that maximized the contact area and increased friction between interfacing stones. Each block was calibrated into the robot's digital workspace using a three-point method based on pre-drilled holes, enabling consistent alignment between the digital and physical models. Minor discrepancies caused by imperfect calibration or uneven base geometry were corrected during assembly through manual adjustment of the plywood plinths. As a result, the final assembly exhibited tight joints with no visible misalignments or gaps.

The assembled arch was exhibited at the Fifteen show at the Bartlett School of Architecture, visited by over 500 visitors. The arch stood stably without adhesives or fasteners, relying

entirely on friction and compressive forces to maintain its structural integrity. The total weight of the completed structure was approximately 120 kilograms, with individual stones averaging around 6 kilograms each. In addition to the primary machined interfaces, four holes were drilled into each mating face during milling to accommodate embedded steel pegs. These pegs provided mechanical reinforcement, improving alignment during assembly while offering increased resistance to shear forces and rotational displacement.

Overall, the prototype arch withstood moderate vibrational forces and manual loading without visible deformation or loosening, demonstrating the effectiveness of the design and fabrication workflow in producing a self-supporting stone structure from irregular material.

4 Conclusion

The results of the prototype confirm the viability of a computational and robotic workflow for producing spanning structures from non-standard stone elements. This approach enabled a minimal-intervention strategy, which preserved the natural morphology of each stone and reduced energy and time associated with machining.

The selected set of stones was constrained to a relative homogenous size and geometry. Future work could look at multi-scalar material sets which significantly increase the complexity of the design process. Further, the material was assumed to have equivalent density and compressive strength. Future work could integrate this material information to further inform the allocation of blocks, for instance allocating larger, denser stones in areas that sit under higher compressive forces.

The integration of a multi-objective optimization routine further supported this goal by balancing face compatibility with alignment along a predefined thrust-line geometry. Although a parabolic curve was used to approximate this thrust line, this simplification may not accurately represent the optimal path of compressive forces. A catenary curve, which better reflects the structural behaviour of dry-stacked systems under uniform load, may improve alignment with physical performance criteria in future iterations. Additionally, the use of only two machined faces per stone limited complexity but constrained the types of geometries that could be achieved.

The robotic milling strategy was generally effective, but limitations in fixturing flexibility required manual adjustment. The current setup, consisting of three repositionable pins and a clamping mechanism, accommodated most stone geometries but could be improved to better handle the full range of irregular forms. Future refinements could include adaptive holding systems or more sophisticated repositioning platforms to minimize setup time.

Manual assembly of the arch, while successful, proved labour-intensive due to the weight of the stones and the precision required for placement. For larger or more complex structures,

the introduction of laser-cut guides, formwork, or adjustable jigs could significantly streamline the process, improving both speed and alignment accuracy. Moreover, robotic methodologies could be developed to automate the assembly process.

Finally, while the physical prototype performed reliably, no formal structural analysis was conducted. The alignment between the final geometry and the intended thrust-line was assessed visually and through tactile inspection. A more rigorous validation such as finite element analysis or thrust-line simulation would be necessary to quantify structural performance, identify stress concentrations, and evaluate long-term behaviour under load.

Despite these limitations, the project successfully demonstrates that irregular, minimally processed stone can be transformed into precise architectural assemblies through a tightly integrated digital-to-physical workflow. The results support the broader potential for computationally optimized and materially efficient stone construction within sustainable architectural practice.

Funding statement - Not Available

5 References

1. Klemm A, Wiggins D. Sustainability of natural stone as a construction material. In: Sustainability of Construction Materials. Elsevier; 2016. p. 283–308.
2. Morel JC, Mesbah A, Oggero M, Walker P. Building houses with local materials: Means to drastically reduce the environmental impact of construction. Build Environ. 2001 Dec;36(10):1119–26.
3. Snethlage R. Natural Stones in Architecture: Introduction. In: Stone in Architecture. Berlin, Heidelberg: Springer Berlin Heidelberg; 2011. p. 1–10.
4. Kerr J, Rayburg S, Neave M, Rodwell J. Comparative Analysis of the Global Warming Potential (GWP) of Structural Stone, Concrete and Steel Construction Materials. Sustainability (Switzerland). 2022 Aug 1;14(15).
5. Rippmann M, Block P. Rethinking structural masonry: Unreinforced, stone-cut shells. Proceedings of Institution of Civil Engineers: Construction Materials. 2013 Dec;166(6):378–89.
6. Kalakoski I, Huuhka S. Spolia revisited and extended: The potential for contemporary architecture. Journal of Material Culture. 2018 Jun 1;23(2):187–213.
7. Önalan B, Mitropoulou I, Triantafyllidis E, Hunhevicz J, De Wolf C. Computational methods for circular design with non-standard materials: Systematic review and future directions. International Journal of Architectural Computing. SAGE Publications Inc.;

2025.

8. Strzałkowski P. Characteristics of waste generated in dimension stone processing. Energies (Basel). 2021 Nov 1;14(21).

9. Tazzini A, Gambino F, Casale M, Dino GA. Managing Marble Quarry Waste: Opportunities and Challenges for Circular Economy Implementation. Sustainability (Switzerland) . 2024 Apr 1;16(7).

10. Jalalian MH, Bagherpour R, Khoshouei M. Wastes production in dimension stones industry: resources, factors, and solutions to reduce them. Environ Earth Sci. 2021 Sep 1;80(17).

11. Çetin S, De Wolf C, Bocken N. Circular digital built environment: An emerging framework. Sustainability (Switzerland). 2021 Jun 1;13(11).

12. Moussavi SM, Svatoš-Ražnjević H, Körner A, Tahouni Y, Menges A, Knippers J. Design based on availability: Generative design and robotic fabrication workflow for non-standardized sheet metal with variable properties. International Journal of Space Structures. 2022 Jun 1;37(2):119–34.

13. Devadass P, Dailami F, Self M. Robotic Fabrication of Non-Standard Material.

14. Clifford B, McGee W, Muhonen M. Recovering Cannibalism in Architecture with a Return to Cyclopean Masonry. Nexus Netw J. 2018 Dec 1;20(3):583–604.

15. Johns RL, Wermelinger M, Mascaro R, Jud D, Gramazio F, Kohler M, et al. Autonomous dry stone. Construction Robotics. 2020 Dec;4(3–4):127–40.

16. Cohen-Steiner D, Alliez P, Desbrun M. Variational shape approximation. In: ACM Transactions on Graphics. 2004. p. 905–14.